

# Atomic Force Microscopy in Detection of Viruses

Norma Hernández-Pedro, Edgar Rangel-López,  
Benjamín Pineda and Julio Sotelo

*Neuroimmunology Unit, National Institute of Neurology and Neurosurgery, Mexico City  
Mexico*

## 1. Introduction

Properties of biological samples, such as DNA, proteins, components of bacterial surfaces and viruses have been studied extensively and provided the driving force for the outstanding progress of detection methods used in cell biology and physiology. Methods like magnetic twisting cytometry, laser-tracking microrheology, magnetic tweezers, the optical stretcher, and various cell indenters; have been used in the study of cell properties, however, imaging resolution has been low. Atomic Force Microscope (AFM) was developed by Binnig, Quate and Gerber in 1986, and since its commercialization, AFM has been a powerful research tool in the scientific community, demonstrating its capability to provide images of biomolecules with high resolution. One of the most important benefits of AFM is the requirement of a minimal amount of sample to perform an accurate diagnostic. Also, AFM does not require staining, labelling, or samples coating, and it is possible to acquire images with minimal pre-treatment in a short time (sometimes minutes). AFM can also be used for real-time and high-resolution imaging of hydrated biological specimens ranging from single molecules to whole cells and tissues.

## 2. Fundamentals of atomic force microscopy (AFM)

AFM is a member of the family of probe microscopes used to scan and characterize surfaces. It generates topographical images from a variety of materials with resolutions of a nanometer (nm) fraction. AFM consists of a microscale rectangular or "V"-shaped cantilever (**Table 1**), typically made of silicon or silicon nitride, with a sharp tip (probe) at its end, with a tip radius of curvature on the order of 50–100 nm. The tip is mounted at the end of a flexible cantilever that serves as a force sensor. The topography of a sample is obtained by measuring and modulating the interaction forces between the tip and the sample, by maintaining a constant tip-sample separation and using Hooke's Law ( $F = -kx$  where  $F$  is force,  $k$  is the spring constant, and  $x$  is the cantilever deflection), the force between the tip and the sample are calculated and derive information about the surface of the sample. The movement of the cantilever is controlled in  $x$ ,  $y$ , and  $z$  axis by piezoelectric crystals. A laser-based optical system is used to track the deflection of the cantilever with respect to the sample surface. As the tip encounters surface features, tiny disturbances in  $z$  cause the cantilever to bend. This movement is amplified by a laser beam focused on the backside of the cantilever that reflects onto a split photodiode, tracing the position of the cantilever.

Cantilever material	Silicon nitride <sup>a</sup>		Silicon <sup>a</sup>
Spring constant( <i>k</i> )	0.58, 0.32, 0.12, 0.06		20-100 N/m
Resonant frequency			200-400 kHz
Cantilever configuration	V-shaped		Single beam
Reflective coating	gold		Uncoated, aluminum
Tip shape	Pyramid	Sphere <sup>b</sup> glass/ polystyrene	Pyramid
Tip radius of curvature/diameter	20-60 nm	0.6-45 μm <sup>b</sup>	5-10 nm
Sidewall angles	35° on all four sides	NA	35° on all four sides

<sup>a</sup>Adapted from SPM Training Notebook (2003).

<sup>b</sup>Parameters from Novascan Technologies.

Abbreviation: NA, not applicable.

Table 1. The Most Common Cantilever Parameters

### 3. Contact and tipping mode to imaging of AFM

The two most common forms of AFM operation are contact and magnetic alternating current (Mac) tapping modes. In contact imaging, sample topography can be measured using constant-height or constant-force settings. In constant-height mode, the distance between the tip and the surface remains fixed during scanning, but the force between the tip and surface changes as the tip encounters surface features. Deflections in the position of the cantilever are used to create an image of the surface. In constant-force mode, the tip remains in contact with the sample using a known applied vertical force as the cantilever scans over the surface. Deflection of the cantilever signals a change in the voltage sent to the z piezo that is adjusted to maintain a constant interaction force between the tip and surface. This voltage sent to the z piezo is converted into height data to create the image. This type of imaging loses the true height information, but it presents more fine details of the sample than the height image because the feedback loop response is faster for correcting the position of the small cantilever. Contact mode is frequently used with hard inorganic surfaces, metals, and for high polymers (with high molecular weight) including polyethylene, silicone and polyurethane elastomers (Siedlecki and Marchant 1998), others uses include fixed cells, proteins, cell surfaces or low modulus biomaterials.

As do other, the Tapping Mode or Mac Mode prevent damage to the soft tip (i.e. on diamond, silicon carbide) is often used for observe molecules, cell surface samples and even dynamic process that occur *in vivo* (Hansma, Cleveland et al. 1994; Moreno-Herrero, Colchero et al. 2004). This method overcomes problems associated with friction, adhesion, electrostatic forces, and other difficulties that conventional AFM scanning methods by alternately placing the tip in contact with the surface to provide high resolution and then lifting the tip off the surface to avoid dragging the tip across the surface, avoiding sample damage by compressing, and tearing. The cantilever vibrates at its resonant frequency under an external electrical excitation, the feedback loop adjusts the oscillation amplitude to restore the original set point value, and a height image can be recorded (Putman, van der Werf et al. 1994; Schindler, Badt et al. 2000). The contrast of a phase image is directly dependent on the elastic properties of the sample.

Applications of Tapping Mode AFM in materials, biomaterials and biology sciences are constantly growing. The commercial technology has improved due to request of users and from experience in acquiring tapping mode data. Some studies show high resolution imaging of molecules such as proteins (Karrasch, Hegerl et al. 1994), channels and receptors on cell surfaces (Muller, Schabert et al. 1995), lipids (Anderton, Lou et al. 2011), and also has been used to imaging living cells; including yeast (Dhadwar, Bemman et al. 2003), neurons (Kondra, Laishram et al. 2009), endothelial cells, virus (Ohnesorge, Horber et al. 1997), and others. Furthermore, important applications of tapping mode include monitoring the action of drugs or other compounds on cells. **Figure 1**

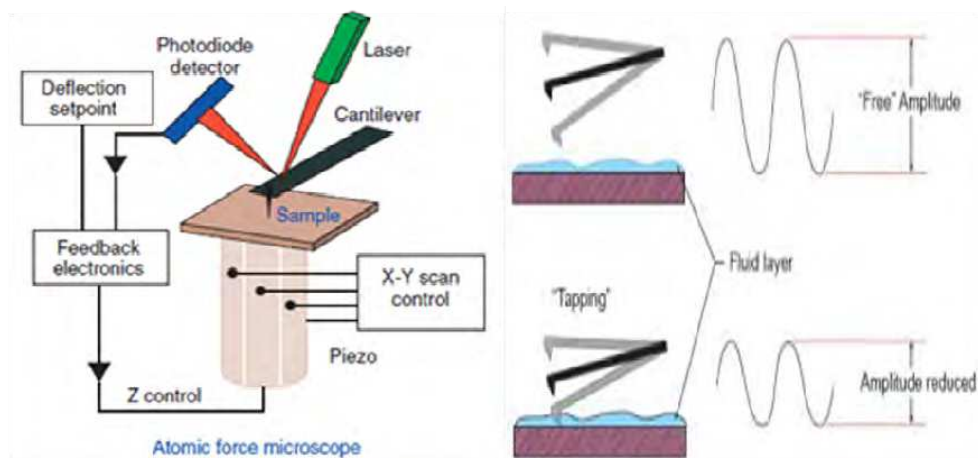


**Fig. 1. Contact mode and tapping mode AFM.** In contact mode imaging is obtained by raster scanning the cantilever and attached probe with respect to the sample surface. Shear forces are applied to the sample during scanning since the probe tip remains in constant contact. In tapping mode, the cantilever is oscillating vertically at high frequency during raster scanning. Interaction of the tip with the sample causes attenuation of the oscillation amplitude, which is used to monitor changes in sample height. Shear forces on the sample are negligible, because the lateral scanning movement of the probe occurs above the sample

#### 4. Sample preparation and fixing

The critical steps in AFM are the sample preparation and surface immobilization, and this is considered the most important aspect to imaging living cells. To fixing the sample is necessary to attach the biomaterial to the sample holder. Substrates that are frequently used include glass cover slips, mica, highly ordered pyrolytic graphite, silicon oxide wafers, and atomically flat gold (Schneeweiss and Rubinstein 2007). The substrate used from AFM depends of the sample that one desires to measure for example, the majority of living cells such as smooth muscle cells, endothelial cells, and fibroblasts, attach well to classical substrates like polystyrene or glass. Other samples, such as those obtained from a cell culture dish, have used gelatine or an extracellular matrix protein like fibronectin and laminin, which can improve the cell attachment (Trache and Meininger 2008). In addition, the use of an adhesive is often required to fix nanoparticles on a substrate. The most common materials used to bond particles to the substrate are Poly-L-lysine, poly-D-lysine,

PEI (poly-ethyleneimide) or APTES (aminopropyltriethoxysilane) (Kasas and Ikai 1995; Wagner 1998; Dufrene 2000; Engel and Muller 2000).

Two drive mechanisms for tapping mode in fluids are available on the multimode AFM. The conventional method of driving the cantilever by acoustic excitation has been joined by a magnetic actuated drive (Putman, 1994). Acoustically driven oscillations of the cantilever in liquid on the multimode AFM occur by excitation of a piezo electric ceramic element in the cantilever holder; however, the sample can move and give erroneous information. The Magnetic Actuated Drive (MAD) mechanism uses an electromagnet in the fluid cell to create a magnetic field to drive specialized event. These probes are coated with a magnetic film (Co or Co/Cr) on the backside (only) to preserve the tip sharpness. It is somewhat easier to identify the resonant frequency of the cantilever when working with the magnetic drive, as the tune shows mainly only the resonant frequency oscillation of the probe. However, the magnetic coating on the backside of the cantilever can lead to the possibility of contamination of sensitive samples with soluble earth and transition metal ions (Revenko and Proksch 2000). Another example that has been developed to diminish the contamination and improve the measurement is the use of like isopore polycarbonate membrane with a pore size comparable to the cell size that is used in a concentrated cell suspension of single bacteria, yeast, or fungal cells under physiological conditions (Kasas and Ikai 1995; Dufrene 2000). Recently, other material like Nanoporous gold (NPG) has been developed for protein immobilization with better results due to its open bi-continuous structure, high surface-to-volume ratio, tunable porosity, chemical stability, and biocompatibility (Tan, Schallom et al. 2011).

## 5. Imaging

AFM images of biomolecules give structural information, as well as information about the material properties of the sample. It is a method with suitable advantages for the study of cell mechanics, by providing high sensitivity, spatial resolution and the ability to be used for real-time measurements (Kirmizis and Logothetidis 2010). The AFM is based on a direct bound to a surface by virtue of a change in local topography allowing a direct mechanical interaction between the probe and the sample. This ability allows the AFM to distinguish between a single monolayer of proteins bound to a surface and multiple layers that result from an interaction between members of an affinity pair. Images often show surface features that are invisible or barely visible in height images or amplitude images (Dufrene 2002).

Imaging surfaces at variables forces set points gives information about the compressibility of the surface as well as characterization of material properties and structure manipulation on the nanometer scale, and visualization and probing of single macromolecules. Some examples to structural parameters measured such as that contained in chromatin fibers (Daban 2011), reconstituted fibers of sequence-defined DNA and core histone octamers on gap junction membranes (Hoh, Lal et al. 1991). Other biomaterials as proteins, DNA molecules, protein-protein complexes, and DNA-protein complexes (Hansma, Sinsheimer et al. 1992; Murphy, Shannon et al. 2011; Shen, Bao et al. 2011) chromosomes (Jondle, Ambrosio et al. 1995; Daban 2011), and cells (Henderson, Haydon et al. 1992) and more recently single RNA molecules (Heus, Puchner et al. 2011) have been measured with AFM.

Other methods, like imaging in air, have been used to visualize cell nuclei disrupted *in situ* (Fritzsche, Schaper et al. 1994; Fritzsche, Schaper et al. 1995), reconstituted fibres of sequence-defined DNA and core histone octamers (Allen, Dong et al. 1993), and soluble

chromatin fibres isolated from hypotonically lysed micrococcal nuclease-treated nuclei (Volkening and Spatz 2009). Inside cells there are some important factors such as the aqueous gel nature of the cytoplasm (Evans and Yeung 1989), heterogeneously distributed actin filaments, intermediate filaments, microtubules (Wang 1998), cell adhesiveness (Pourati, Maniatis et al. 1998), or the presence of nucleus and other organelles (Petersen, McConnaughey et al. 1982) which could affect the mechanical properties of the cells. **Table 2**

	<b>Protein Structures</b>	<b>Function</b>	<b>Citation</b>
<b>Molecular motors</b>	F-adenosine triphosphate (ATP) synthase rotors	Synthases use the energy of a transmembrane proton	Seelert et al., 2000 and Stahlberg et al., 2001
	The f29 rotary motor	Converts a mechanical rotation to a translational movement of DNA	Simpson et al, 2000
<b>Ion pumps and channels</b>	Bacteriorhodopsin	Converts the energy of "green" light(500–650 nm) into an electrochemical proton gradient	Haupts U et al 1999
	Halorhodopsin	showed neighbored tetramers to be orientated with their extracellular and cytoplasmic surface towards the membrane surface	Persike et al., 2001 and Kolbe et al., 2000
	Potassium channel	Stabilize membrane potential	van Huizen et al., 1999
<b>Membrane channels</b>	Aquaporin1 (AQP1)	Channel proteins that transporting water and other metabolites	Pohl et al., 2001
	Major intrinsic protein (AQP0)	Intrinsic protein expressed in eye lens fiber cells	Fotiadis et al., 2000
<b>Proteins involved into photosynthesis</b>	Photosystem I	Oxygenic photosynthesis in cyanobacteria and plants	Fotiadis et al., 1998
	Light-harvesting-complex 2	Transfers excitation energy to the light-harvesting complex 1	Scheuring et al., 2001
<b>Toxins</b>	Cholera toxin	Causes the enzymatic subunit to be clipped from the rest of the protein and transferred into the cell	Mou et al., 1995; and Yang et al., 1993
	Cry1Aa	Forms toxic pores	Vie et al., 2001
	a-hemolysin	Create water-filled channels that lead to cell death and lysis	Czajkowsky et al., 1998 and Song et al., 1996
	VacA	Induces vacuolation of acidic intracellular components	Czajkowsky et al., 1999 and Iwamoto et al., 1999
<b>Chaperonins and proteasomes</b>	GroE chaperone system	Chaperone machinery	Mou et al., 1996, 1996
	20 S proteasome	Degrades misfolded or regulatory proteins	Dorn et al., 1999
<b>Cellulose</b>		Unbranched polymer of glucose residues joined	Baker et al., 1997; Baker et al., 2000

Table 2. Some Applications of Atomic Force Microscopy

## 6. Virus detection by AFM

Historically, the optical microscope and the electron microscope (EM) have played a key role in the discovery and structural characterization of viral isolates (Biel and Gelderblom 1999; Hazelton and Gelderblom 2003). Today, EM is used mainly as a research tool and not in main stream routine diagnoses because it is not suited for high through-put analyses. For routine virus detection and monitoring the spread of disease, most available diagnostic methods rely almost exclusively on polymerase chain reaction (PCR) or enzyme-linked immunosorbent assay (ELISA). Identification and measurement of viral DNA or RNA is provided by PCR, whereas viral proteins and antiviral antibodies detection are made by ELISA (Belak and Thoren 2001; Henrickson 2004; Madeley 2004; Olofsson, Brittain-Long et al. 2011). The inconvenience of these techniques is that they do not measure complete particles and they are indirect indicators of viral load. Also, in conditions where viral latency has been established, the ability to directly monitor recurrences through the measurement of intact viral particles would be a great asset for the clinical setting. The early and correct diagnosis of viral infection is also relevant, especially in severe infections such as atypical herpes virus infections, in order to ensure effective treatment of the disease and prevention of complications (Hawrami and Breuer 1999; Pineda, Saniger et al. 2009). The use of new tools such as AFM could play an important role in the clinical or epidemiological setting when critical situations require a rapid diagnosis, for example the recent H1N1 influenza epidemic experienced in the United States and Mexico (Tian, Wang et al. 2011) where AFM could be the only method available that allows morphological identification by direct visualization of intact particles.

## 7. Viruses morphology

Viruses are grouped on the basis of size and shape, chemical composition, structure of the genome, and mode of replication. Viral genomes are surrounded and protected by a protein shell, the capsid. The type of capsid has been used to classify viruses in three main groups: Helical symmetry, Virus Core Structure and Icosahedral Symmetry. Some techniques, like X-ray diffraction and cryo-electron microscopy, have been used to determine the structure of viral capsids providing a good resolution. Nevertheless, the use of AFM has allowed the discovery of new structures, obtaining higher resolution, and physical characteristics of the capsid. In the next sections, we give some examples of AFM measurement according to their capsid classification.

### 7.1 Helical symmetry

A fundamental parameter for virus particles is their symmetry. Helical viruses are defined by their pitch; a single type of capsomer stacked around a central axis to form a helical structure and the protein of the coat has exactly the same orientation (Gelderblom 1996). The symmetric shapes allow to use the same component protein multiple times to create large structures from a minimum number of distinct protein species.

The Tobacco Mosaic Virus (TMV) has a variety of organized structures, such as the disk aggregate and helical rod, which play distinct roles in the genesis of the virus during infection (Sachse, Chen et al. 2007). This virus infects plants which will often displays developmental abnormalities that include stunting, leaf curling, and the loss of apical dominance. The TMV is the typical member of the Tobamovirus genus in the Virgaviridae

family and is one of the most studied viruses by AFM (Dawson, Beck et al. 1986). TMV virion, measured by AFM, consists of approximately 2,130 identical coat proteins helically wrapped around a 6.4 kb positive strand of genomic mRNA, making it an 18 nm diameter and 300 nm long rigid nanotube with a 4 nm diameter inner channel (Culver 2002; Michel, Ivanovska et al. 2006). Recently, other structures were identified in TMV by AFM, such as the satellite tobacco mosaic virus characterized by RNA helical segments, where, RNA base sequence, therefore, may be sufficient to encode the conformation of the encapsidated RNA even in the absence of coat proteins (Day, Kuznetsov et al. 2001).

Another important virus is influenza. This is a member of orthomyxoviridae family, and it has three members: influenza virus A, B, and C. Influenza A virus, both seasonal and pandemic, has the potential to cause rampant the devastation disease around the world. Influenza A uses its RNA during impregnation and causes a subsequent infection, which is characterized primarily by pulmonary affection that may advance to an acute pulmonary respiratory failure. Influenza type A is the most studied by AFM and some studies exhibit a surface topography that is characterized by rugged features and gear-like protuberances (Liu, Hu et al. 2008). Also, surface morphology is characterized by the presence of large nanoparticles, typically 120 to 250 nm wide at the base and 50 to 100 nm tall. Now, it is known that the influenza virus is a quasi-spherical object, approximately of 100 to 120 nm in diameter (Wickramasinghe, Kalbfuss et al. 2005).

Ebola and Marburg viruses are prime examples of emerging pathogens; they cause fatal hemorrhagic fever in humans. Identification of major determinants of the Ebola virus pathogenicity has been hampered by the lack of effective strategies for experimental mutagenesis. Recent discoveries suggest that filoviruses, along with other phylogenetically or functionally related viruses, utilize a complex mechanism of replication exploiting multiple cellular components including lipid rafts, endocytic compartments, and vacuolar protein sorting machinery (Aman, Bosio et al. 2003). The single-stranded negative-sense RNA genome is encased in a nucleocapsid complex, which consists of the following four viral proteins: the nucleoprotein (NP), the viral proteins (VP35 and VP30) and the polymerase (L). This complex is surrounded by a matrix consisting of VP40 and VP24, which is packaged by a lipid membrane envelope obtained during budding from the host cell. The envelope is composed of the glycoprotein (GP) protein, which is post-translationally cleaved by a furin protease into two fragments, GP1 and GP2, although this cleavage is not necessary for *in vitro* viral infection of cells (Wool-Lewis and Bates 1999; Neumann, Feldmann et al. 2002). Ebola fusion peptide interacts with living cells, and its capacity to induce cell fusion is decreased in cholesterol-depleted cells. Force spectroscopy based on AFM assays reveals a pattern of high affinity force when the Ebola fusion peptide interacts with membrane rafts. It is also observed that the peptide is able to induce aggregation of the lipid rafts, suggesting an important role for phosphatidylinositol and cholesterol during entry of the virus into the target cells (Suarez, Gomara et al. 2003).

## 7.2 Virus core structure

Except for helical nucleocapsids, little is known about the packaging or organization of the viral genome within the core. Small virions are simple nucleocapsids containing 1 to 2 protein species. The larger viruses contain within the core the nucleic acid genome complexed with basic proteins and are protected by a single- or double layered capsid or by an envelope (Gelderblom 1996).

Isolated human immunodeficiency virus (HIV) and HIV-infected human lymphocytes in culture have been imaged for the first time by atomic force microscopy. Purified virus particles spread on glass substrates are roughly spherical, reasonably uniform, though pleomorphic in appearance, and have diameters of about 120 nm. Similar particles are also seen on infected cell surfaces, but morphologies and sizes are considerably more varied, which is possibly a reflection of the budding process. The surfaces of HIV particles exhibit filaments of protein, presumably GP120, which do not physically resemble spikes. The protein filaments, which number about 100 per particle, have average diameters of about 200 Å, nonetheless, they have a large size variance. They likely consist of arbitrary associations of small numbers of GP120 monomers on the surface. Examining several hundred of virus particles, authors found no evidence that the GP120 monomers form trimmer based on three fold symmetry (Kuznetsov, Victoria et al. 2003).

Hepatitis B, is a virus consists of an inner nucleocapsid or core, surrounded by a lipid envelope containing virally encoded surface proteins, it is member of the taxonomic family hepadnaviridae and still poses a major health threat; it causes hepatitis, liver cancer, and liver cirrhosis. Direct measurements with AFM revealed morphological changes upon maturation through induced and heat-/storage-incurred oxidative refolding. Particle uniformity and regularity was greatly improved, and protrusions formed by the protein subunits were more prominent on the surface of the mature particles. Decreased conformational flexibility in the mature surface antigen of Hepatitis B virus (rHBsAg) particles was demonstrated. Both the accessible hydrophobic cavities under native conditions and the changeable hydrophobic cavities upon denaturant-induced unfolding showed substantial decrease upon maturation of the rHBs Ag particles. These changes in the structural properties may be critical for the antigenicity and immunogenicity of this widely-used vaccine component (Zhao, Wang et al. 2006).

Vaccinia virus, a characterized member of the Poxviridae family, is unusual among most double-stranded DNA viruses in that both viral transcription and replication occur in the cytoplasm of the host cell (Condit, Moussatche et al. 2006). Poxviridae virus is generally shaped like a brick or as an oval form, similar to a rounded brick because they are wrapped by the endoplasmic reticulum (Holowczak 1982). The virion is exceptionally large; its size is around 200 nm in diameter and 300 nm in length and carries its genome in a single, linear, double-stranded segment of DNA (Dales and T. 1981; Fenner, Wittek et al. 1989; Moss 1991). This virus has relevance because of its historical role in smallpox eradication, and its relatively benign tropism and is one of the largest viruses to replicate in humans are reasons that explains why is the most studied virus in this family. The viral DNA genome is linear, double stranded. The Copenhagen strain is 191 kbp in length and contains at least 266 open reading frames (Goebel, Johnson et al. 1990; Johnson, Goebel et al. 1993). Kuznetsov et al characterized the shape, dimensions, and general surface characteristics of hydrated vaccinia mature virus. The virus assumes a familiar rectangular shape upon dehydration while particles were pleomorphic with an outer surface design varying from the more regular, short, haphazardly, intersecting to railroad tracks topography. Removal of the outer lipid/protein membrane on vaccinia, a layer of 20 to 40 nm in thickness, was encountered that was composed of fibrous elements. Beneath this layer were the virus core and its prominent lateral bodies. The core, in addition to the lateral bodies, was composed of a thick, multilayered shell of proteins of several sizes and shapes. The shell was thoroughly permeated with pores, or channels. The DNA was readily visualized by AFM, revealing

some regions to be “soldered” by proteins, others to be heavily complexed with protein, and yet other parts to apparently exist as bundled, naked DNA (Kuznetsov, Gershon et al. 2008). Also, the Poxviridae virus, characterized by AFM in an aqueous environment, shows a fairly regularly repeating pairs of rodshaped structures with a total width of 7-11 nm and a length of 60-90 nm (Ohnesorge, Horber et al. 1997).

In 2003, Malkin et al, described by AFM intact intracellular mature vaccinia virus (IMV), virions, as well as the chemical and enzymatic treatment products thereof. In their observations, they described virion cores, core-enveloping coats, and core substructures of the vaccinia virus. The AFM imaging of core substructures indicated an association of the linear viral DNA genome with a segmented protein sheath forming an extended around 16 nm-diameter filament with helical surface topography; enclosure of this filament within a 30 to 40-nm-diameter tubule which also shows helical topography; and enclosure of the folded, condensed 30 to 40-nm-diameter tubule within the core by a wall covered with peg-like projections. The size of the isolated virions was 70 to 100-nm-diameter particles (Malkin, McPherson et al. 2003).

### 7.3 Icosahedral symmetry

An icosahedron is a polyhedron having 20 equilateral triangular faces and 12 vertices. Lines through opposite vertices define axes of fivefold rotational symmetry: all structural features of the polyhedron repeat five times within each 360° of rotation about any of the fivefold axes. Lines through the centers of opposite triangular faces form axes of threefold rotational symmetry; twofold rotational symmetry axes are formed by lines through midpoints of opposite edges. An icosahedron (polyhedral or spherical) with fivefold, threefold, and twofold axes of rotational symmetry is defined as having 532 symmetry (Gelderblom 1996).

Various surfaces, proteins, and RNA are identifiable by AFM. Marek’s disease virus (MDV) is one of the most potent oncogenic alpha herpes viruses, leads to highly contagious immunosuppressive and neoplastic disease in susceptible chickens and less commonly turkeys and quails (Federica Giardi, La Torre et al. 2009). It is the etiologic agent of Marek’s disease (MD), which is a highly contagious malignant lymphoma that causes dullness with progression of T-lymphomas and finally ataxia and paralysis (Morimura, Ohashi et al. 1998). Di Bucchianico et al investigated the different structure of chromatin in chromosome aberrations due to MDV insertion. They found a duplication [78,WZ,dup(1p)(p22-p23)] and a deletion [78,WZ,cht del(3)(q2.10)] of chromosomes 1 and 3 (Di Bucchianico, Giardi et al. 2010). The architecture of chromosomes observed by AFM can be related to the data obtained with classic banding techniques. Also, evidence the presence of chromatin bridges between sisters and deletions of chromatid regions. The deletions of the two chromatids have a size of 100 and 50 nm, respectively (Di Bucchianico, Giardi et al. 2011).

RNA molecules are other structures investigated by AFM, and this is important due to a small amount of RNA in icosahedral viruses (Kuznetsov, Daijogo et al. 2005). Poliovirus and turnip yellow mosaic virus (TYMV) are monopartite viruses, containing a positive-strand RNA, which infects crucifers (broccoli, cauliflower, radishes, and several green vegetables) (Weiland and Dreher 1993). Kuznetsov et al, studied RNA in different conditions and found a uniform spherical inside of virion to approximately 20 nm. After 30 minutes to an hour, the spherical particles lose their integrity, assume an irregular banded

fiber appearance, segment into secondary structural domains and finally single-stranded RNA connecting secondary structural domains (Kuznetsov, Daijogo et al. 2005).

Paramecium bursaria chlorella virus type 1 (PBCV-1) is a member of large group “Phycodnaviridae viruses” that infect eukaryotic cells. The highest resolution AFM images have revealed a protein surface network; an individual trimetric capsid protein as well as their subunits displayed about the central threefold axis. The shapes of the subunits and their arrangements are most consistent. This AFM study also provides information on the structure of the PBCV-1 that is involved in virus infection. A distinctive pentamer of five unique proteins occurs in fivefold vertex, along with another distinctive protein exactly in the center of the homopentamer. This apical protein is unusual in that it appears sensitive to mechanical force and retracts into the interior of the virion (Kuznetsov, Gurnon et al. 2005).

Mason–Pfizer monkey virus (M-PMV) is a type D retrovirus which pre-assembles immature capsids in the cytoplasm prior to transport to the host cell membrane where they are released. Maturation then takes place. Bacteria expressing M-PMV Gag protein, and various truncated forms of Gag, produce spherical particles within inclusion bodies, and these exhibit features suggestive of icosahedral symmetry (Nermut, Hockley et al. 1998). Particles of  $\Delta$ ProCANC, a fusion of capsid (CA) and nucleocapsid (NC) proteins of Mason–Pfizer monkey virus (M-PMV), which lacks the proline amino terminal, were reassembled *in vitro* and visualized by AFM. The particles, 83–84 nm in diameter, exhibited ordered domains based on trigonal arrays of prominent rings with center to center distances of 8.7 nm. Imperfect closure of the lattice on the spherical surface was affected by formation of discontinuities. The lattice is consistent only with plane group p3 where one molecule is shared between contiguous rings. There are no pentameric clusters or evidence that the particles are icosahedral. Tubular structures were also reassembled, *in vitro*, from two HIV fusion proteins,  $\Delta$ ProCANC and CANC. The tubes were uniform in diameter, 40 nm, but varied in length to a maximum of 600 nm. They exhibited left handed helical symmetry based on a p6 hexagonal net (Kuznetsov, Ulbrich et al. 2007).

Herpes viruses are a leading cause of human viral disease, after the influenza and cold viruses. They are capable of causing overt disease or remain silent for many years only to be reactivated. This reflects the creeping or spreading nature of the skin lesions caused by many herpes virus types. Herpes simplex virus type 1 (HSV1) virions encapsulate their 152 kbp double-stranded DNA genome in an icosahedral capsid that is surrounded by an amorphous protein layer, called the tegument, and a lipid-containing envelope. Assembly of herpes viruses is initiated in the nucleus where procapsids self-assemble around a protein scaffold and subsequently mature. Ross et al, determined structural changes during maturation of virus and DNA packaging by AFM. Atomic force microscopy experiments revealed that A and C capsids were mechanically indistinguishable, indicating that the presence of DNA does not account for changes in mechanical properties during capsid maturation (Roos, Radtke et al. 2009).

## 8. Solid-phase assay for detection of varicella zoster virus by AFM

We performed an study regarding the detection of varicella zoster virus using a novel Bionanotechnological approach that couples atomic force microscopy with high affinity solid phase capture of viral particles called Virichip® (Pineda, Saniger et al. 2009).

Many general features of virus architecture are readily apparent from a variety of studies; high resolution AFM allows the discrimination of viruses based on their size and shape in a process that does not require staining, fixing or other synthetic preparations. This technique has been used successfully to diagnose viral infections such as West Nile virus, herpes viruses, retroviruses and poxviruses. These enabling properties of AFM combined with solid phase immunocapture of virus particles make possible a multi-tiered detection and identification assay with potential use in rapid pathogen diagnosis.

Afterwards, Nettikadan et al, developed a solid phase and affinity substrate called Virichip® which consists in a microarray of viral proteins on a fresh gold-coated silicon surface; this is incubated with recombinant protein A/G to generate a surface capable to bind and orientate monoclonal antibodies. The first detection of virus using ViriChip platform and AFM was made to detect canine parvovirus virus-like particles (CPV), Coxsackie virus B3 Nancy (CB3), and one morphologically distinct linear helical virus, bacteriophage fd (Nettikadan, Johnson et al. 2003).

The rapid detection and identification of pathogens is critically important to minimize the transfer and spread of diseases and to devise and evaluate effective treatment strategies. For example, Varicella Zoster virus (VZV) detection is clinically important, however the techniques used to detect this disease have disadvantages, including false positive and negative results, the use of specialized and expensive equipment and the need of expert personal performance. At present, the serological methods for the detection of antibodies (either IgG or IgM) are sometimes used to confirm the diagnosis, however, patients who are immuno-supressed or immuno-compromised may have VZV infection without any detectable antibodies.

Varicella ViriChip® construction (VVC) is a sensitive, specific and quick method that allows the visualization of the virus, the specific detection by immunological means and the recovery of virus particles for further analysis. The method does not require additional steps, and a minimal quantity obtained from a vesicle fluid from cutaneous VZV lesions is a sufficient amount to discriminate between VZV and other common pathogens. Additionally, VVC allows sample transportation for further analysis and now Portable AFMs are already available (Pineda, Sanigeret al. 2009) (see Figure 2).



Fig. 2. **Virus distribution on the VVC.** Distribution of the virus in the VVC domain is indicated by the fluorescent antibodies against varicella zoster virus. The target area (circle) has a diameter of 600  $\mu\text{m}$ .

The importance of Virichip is its ability to detect whole virus particles and identify them using two integrated sets of criteria without damaging the virus or its genome. First, the dimensional properties of the captured particles as determined by AFM should be in agreement with those for the *family* of viruses suspected, and second, the capture by a type specific antibody indicates positive type-specific interaction. The combination of these properties should permit placement of a virus within a *family*, sub-family and a serotype depending on the nature of the epitope recognized by the capture antibody<sup>79</sup>. Currently, the AFM has a sensitivity of  $10^3$  TCID<sub>50</sub>  $\mu\text{l}^{-1}$ . In contrast, ELISA-based detection using the same antibodies has a detection limit of only 107 plaque forming units. Furthermore, although RT-PCR is reportedly more sensitive ( $\sim 0.1$  TCID<sub>50</sub>), RTPCR measures only the presence of RNA and provides no information as to the bioinfectivity in the sample or whether there are even virus particles present (Straub, Pepper et al. 1994; Metcalf, Melnick et al. 1995). The use of Virichip® allows the rapid detection of the virus and it requires a minimal quantity of sample. VVC allows the rapid detection of the virus and it diminishes the handling time, the risks of cross-contamination, and the probability of false positive results (see Figure 3 and 4).

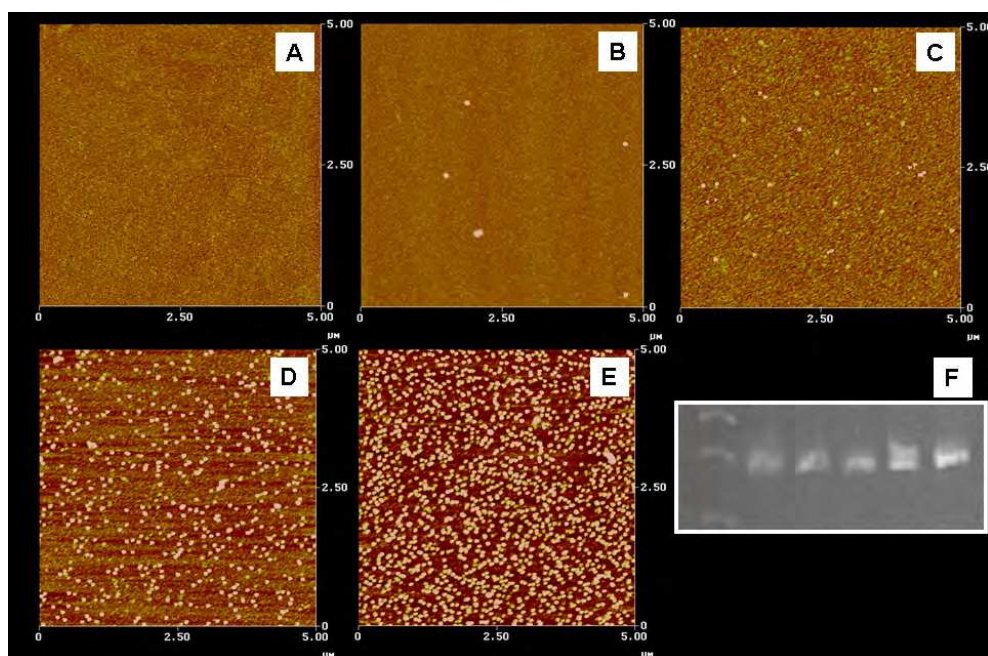


**Fig. 3. Tenfold serial dilutions of VZV over the chip surfaces and its correlation with conventional PCR.** Virus particles from  $1\mu\text{l}$  of 10-fold serial dilutions ranging from  $10^5$  viral particles of VZV were captured on a chip and used as templates to determine the VVZ sensitivity comparing it to PCR. (A)  $10^1$  (1:100,000 dilution). (B)  $10^2$  (1:10,000 dilution). (C)  $10^3$  (1:1,000 dilution). (D)  $10^4$  (1:100 dilution). (E)  $10^5$  (1:10 dilution). (F) PCR amplification of each Virichip, from left to right: lane 1, molecular weight marker (MWM), lanes 2-6 show amplification of the virus chips containing from  $10^1$  to  $10^5$  copies of VZV. The signal intensity in the agarose 2% gel appeared to be proportional to the virus concentration. The sensitivity of this detection method was  $10^2$  viral particles/ $\mu\text{l}$ .

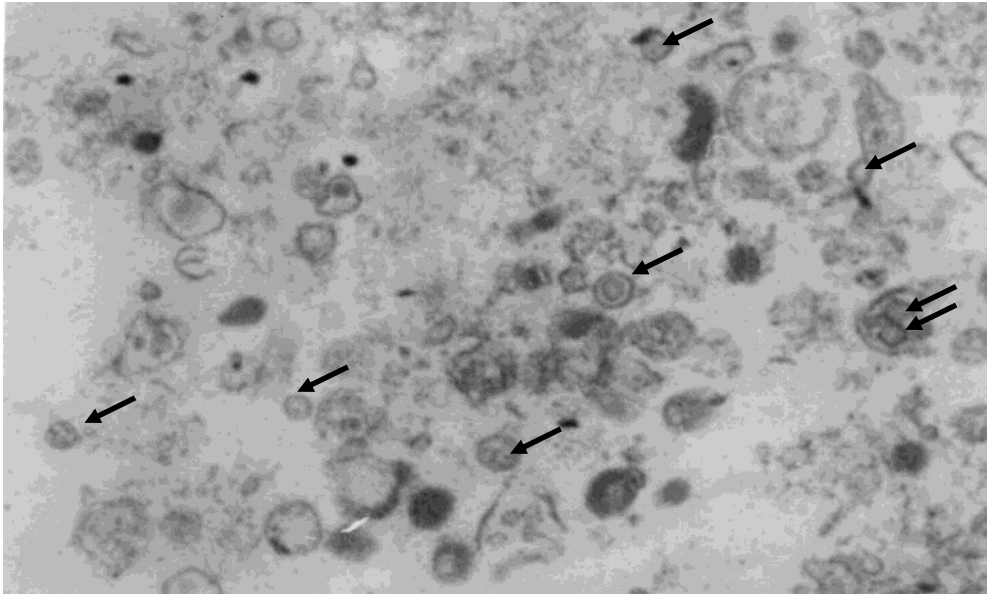


Fig. 4. **Electron microscopy appearances of VZV particles.** The viral particles were eluted from the ViriChip and concentrated by ultracentrifugation. The image shows enveloped and non-enveloped virions containing dense cores. The size of the virus with the capsomere ranges between 80-120 nm and with the envelope between 180-200 nm.

## 9. Conclusions

The AFM has many advantages as it is a simple and relatively inexpensive technique; it is more portable than SEM or TEM; requires a minimal quantity of sample for measurements, and can be linked with other molecular techniques, such as PCR or EM, with efficient results. The method does not damage the virus or its genome, allowing the detection of whole virus particles and the possibility to identify the family, sub-family, serotype and other complex structures. Also, the Virichip® allows the rapid detection of the VVZ, reduces handling time, risks of cross-contamination, and the probability to detect false positives; making it an attractive clinical diagnostic tool in the virology field. The combination the AFM visualization with immunocapture and molecular biology methods is a useful tool for the identification, determination of diagnosis, and the monitoring of many virus infections. The Virichip® is a novel and promising method that could be used to increase the acquaintance and treatment of diseases caused by virus infections.

## 10. References

- Allen, M. J., X. F. Dong, et al. (1993). "Atomic force microscope measurements of nucleosome cores assembled along defined DNA sequences." *Biochemistry* 32(33): 8390-8396.
- Aman, M. J., C. M. Bosio, et al. (2003). "Molecular mechanisms of filovirus cellular trafficking." *Microbes Infect* 5(7): 639-649.

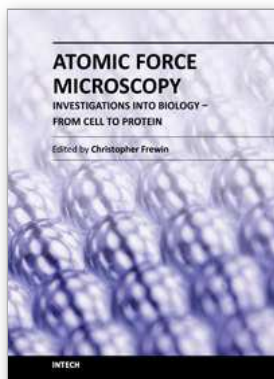
- Anderton, C. R., K. Lou, et al. (2011). "Correlated AFM and NanoSIMS imaging to probe cholesterol-induced changes in phase behavior and non-ideal mixing in ternary lipid membranes." *Biochim Biophys Acta* 1808(1): 307-315.
- Belak, S. and P. Thoren (2001). "Molecular diagnosis of animal diseases: some experiences over the past decade." *Expert Rev Mol Diagn* 1(4): 434-443.
- Biel, S. S. and H. R. Gelderblom (1999). "Diagnostic electron microscopy is still a timely and rewarding method." *J Clin Virol* 13(1-2): 105-119.
- Condit, R. C., N. Moussatche, et al. (2006). "In a nutshell: structure and assembly of the vaccinia virion." *Adv Virus Res* 66: 31-124.
- Culver, J. N. (2002). "Tobacco mosaic virus assembly and disassembly: determinants in pathogenicity and resistance." *Annu Rev Phytopathol* 40: 287-308.
- Daban, J. R. (2011). "Electron microscopy and atomic force microscopy studies of chromatin and metaphase chromosome structure." *Micron* 42(8): 733-750.
- Dales, S. and P. B. G. T. (1981). "Biology of poxviruses. Virology monographs." Springer-Verlag.
- Dawson, W. O., D. L. Beck, et al. (1986). "cDNA cloning of the complete genome of tobacco mosaic virus and production of infectious transcripts." *Proc Natl Acad Sci U S A* 83(6): 1832-1836.
- Day, J., Y. G. Kuznetsov, et al. (2001). "Biophysical studies on the RNA cores of satellite tobacco mosaic virus." *Biophys J* 80(5): 2364-2371.
- Dhadwar, S. S., T. Bemman, et al. (2003). "Yeast cell adhesion on oligopeptide modified surfaces." *Biotechnol Adv* 21(5): 395-406.
- Di Bucchianico, S., M. F. Giardi, et al. (2010). "Cytogenetic stability of chicken T-cell line transformed with Marek's disease virus: atomic force microscope, a new tool for investigation." *J Mol Recognit*.
- Di Bucchianico, S., M. F. Giardi, et al. (2011). "Cytogenetic stability of chicken T-cell line transformed with Marek's disease virus: atomic force microscope, a new tool for investigation." *J Mol Recognit* 24(4): 608-618.
- Dufrene, Y. F. (2000). "Direct characterization of the physicochemical properties of fungal spores using functionalized AFM probes." *Biophys J* 78(6): 3286-3291.
- Dufrene, Y. F. (2002). "Atomic force microscopy, a powerful tool in microbiology." *J Bacteriol* 184(19): 5205-5213.
- Engel, A. and D. J. Muller (2000). "Observing single biomolecules at work with the atomic force microscope." *Nat Struct Biol* 7(9): 715-718.
- Evans, E. and A. Yeung (1989). "Apparent viscosity and cortical tension of blood granulocytes determined by micropipet aspiration." *Biophys J* 56(1): 151-160.
- Federica Giardi, M., C. La Torre, et al. (2009). "Effects of transferrins and cytokines on nitric oxide production by an avian lymphoblastoid cell line infected with Marek's disease virus." *Antiviral Res* 81(3): 248-252.
- Fenner, F., R. Wittek, et al. (1989). "The orthopoxviruses. ." Academic Press, Inc., New York, N.Y.
- Fritzsche, W., A. Schaper, et al. (1994). "Probing chromatin with the scanning force microscope." *Chromosoma* 103(4): 231-236.
- Fritzsche, W., A. Schaper, et al. (1995). "Scanning force microscopy of chromatin fibers in air and in liquid." *Scanning* 17(3): 148-155.
- Gelderblom, H. R. (1996). "Structure and Classification of Viruses."

- Goebel, S. J., G. P. Johnson, et al. (1990). "The complete DNA sequence of vaccinia virus." *Virology* 179(1): 247-266, 517-263.
- Hansma, H. G., R. L. Sinsheimer, et al. (1992). "Atomic force microscopy of single- and double-stranded DNA." *Nucleic Acids Res* 20(14): 3585-3590.
- Hansma, P. K., J. P. Cleveland, et al. (1994). Tapping mode atomic force microscopy in liquids, AIP.
- Hawrami, K. and J. Breuer (1999). "Development of a fluorogenic polymerase chain reaction assay (TaqMan) for the detection and quantitation of varicella zoster virus." *J Virol Methods* 79(1): 33-40.
- Hazelton, P. R. and H. R. Gelderblom (2003). "Electron microscopy for rapid diagnosis of infectious agents in emergent situations." *Emerg Infect Dis* 9(3): 294-303.
- Henderson, E., P. G. Haydon, et al. (1992). "Actin filament dynamics in living glial cells imaged by atomic force microscopy." *Science* 257(5078): 1944-1946.
- Henrickson, K. J. (2004). "Advances in the laboratory diagnosis of viral respiratory disease." *Pediatr Infect Dis J* 23(1 Suppl): S6-10.
- Heus, H. A., E. M. Puchner, et al. (2011). "Atomic force microscope-based single-molecule force spectroscopy of RNA unfolding." *Anal Biochem* 414(1): 1-6.
- Hoh, J. H., R. Lal, et al. (1991). "Atomic force microscopy and dissection of gap junctions." *Science* 253(5026): 1405-1408.
- Holowczak, J. A. (1982). "Poxvirus DNA." *Curr Top Microbiol Immunol* 97: 27-79.
- Johnson, G. P., S. J. Goebel, et al. (1993). "An update on the vaccinia virus genome." *Virology* 196(2): 381-401.
- Jondle, D. M., L. Ambrosio, et al. (1995). "Imaging and manipulating chromosomes with the atomic force microscope." *Chromosome Res* 3(4): 239-244.
- Karrasch, S., R. Hegerl, et al. (1994). "Atomic force microscopy produces faithful high-resolution images of protein surfaces in an aqueous environment." *Proc Natl Acad Sci U S A* 91(3): 836-838.
- Kasas, S. and A. Ikai (1995). "A method for anchoring round shaped cells for atomic force microscope imaging." *Biophys J* 68(5): 1678-1680.
- Kirmizis, D. and S. Logothetidis (2010). "Atomic force microscopy probing in the measurement of cell mechanics." *Int J Nanomedicine* 5: 137-145.
- Kondra, S., J. Laishram, et al. (2009). "Integration of confocal and atomic force microscopy images." *J Neurosci Methods* 177(1): 94-107.
- Kuznetsov, Y., P. D. Gershon, et al. (2008). "Atomic force microscopy investigation of vaccinia virus structure." *J Virol* 82(15): 7551-7566.
- Kuznetsov, Y. G., S. Daijogo, et al. (2005). "Atomic force microscopy analysis of icosahedral virus RNA." *J Mol Biol* 347(1): 41-52.
- Kuznetsov, Y. G., J. R. Gurnon, et al. (2005). "Atomic force microscopy investigation of a chlorella virus, PBCV-1." *J Struct Biol* 149(3): 256-263.
- Kuznetsov, Y. G., P. Ulbrich, et al. (2007). "Atomic force microscopy investigation of Mason-Pfizer monkey virus and human immunodeficiency virus type 1 reassembled particles." *Virology* 360(2): 434-446.
- Kuznetsov, Y. G., J. G. Victoria, et al. (2003). "Atomic force microscopy investigation of human immunodeficiency virus (HIV) and HIV-infected lymphocytes." *J Virol* 77(22): 11896-11909.

- Liu, Y. F., K. X. Hu, et al. (2008). "[Study on the morphology of influenza virus A by atomic force microscopy]." *Bing Du Xue Bao* 24(2): 106-110.
- Madeley, C. R. (2004). "Molecular and diagnostic clinical virology in real time." *Clin Microbiol Infect* 10(5): 471; author reply 471-472.
- Malkin, A. J., A. McPherson, et al. (2003). "Structure of intracellular mature vaccinia virus visualized by in situ atomic force microscopy." *J Virol* 77(11): 6332-6340.
- Metcalf, T. G., J. L. Melnick, et al. (1995). "Environmental virology: from detection of virus in sewage and water by isolation to identification by molecular biology--a trip of over 50 years." *Annu Rev Microbiol* 49: 461-487.
- Michel, J. P., I. L. Ivanovska, et al. (2006). "Nanoindentation studies of full and empty viral capsids and the effects of capsid protein mutations on elasticity and strength." *Proc Natl Acad Sci U S A* 103(16): 6184-6189.
- Moreno-Herrero, F., J. Colchero, et al. (2004). "Atomic force microscopy contact, tapping, and jumping modes for imaging biological samples in liquids." *Phys Rev E Stat Nonlin Soft Matter Phys* 69(3 Pt 1): 031915.
- Morimura, T., K. Ohashi, et al. (1998). "Pathogenesis of Marek's disease (MD) and possible mechanisms of immunity induced by MD vaccine." *J Vet Med Sci* 60(1): 1-8.
- Moss, B. (1991). "Vaccinia virus: a tool for research and vaccine development." *Science* 252(5013): 1662-1667.
- Muller, D. J., F. A. Schabert, et al. (1995). "Imaging purple membranes in aqueous solutions at sub-nanometer resolution by atomic force microscopy." *Biophys J* 68(5): 1681-1686.
- Murphy, P. J., M. Shannon, et al. (2011). "Visualization of recombinant DNA and protein complexes using atomic force microscopy." *J Vis Exp*(53).
- Nermut, M. V., D. J. Hockley, et al. (1998). "Further evidence for hexagonal organization of HIV gag protein in prebudding assemblies and immature virus-like particles." *J Struct Biol* 123(2): 143-149.
- Nettikadan, S. R., J. C. Johnson, et al. (2003). "Virus particle detection by solid phase immunocapture and atomic force microscopy." *Biochem Biophys Res Commun* 311(2): 540-545.
- Neumann, G., H. Feldmann, et al. (2002). "Reverse genetics demonstrates that proteolytic processing of the Ebola virus glycoprotein is not essential for replication in cell culture." *J Virol* 76(1): 406-410.
- Ohnesorge, F. M., J. K. Horber, et al. (1997). "AFM review study on pox viruses and living cells." *Biophys J* 73(4): 2183-2194.
- Olofsson, S., R. Brittain-Long, et al. (2011). "PCR for detection of respiratory viruses: seasonal variations of virus infections." *Expert Rev Anti Infect Ther* 9(8): 615-626.
- Petersen, N. O., W. B. McConnaughey, et al. (1982). "Dependence of locally measured cellular deformability on position on the cell, temperature, and cytochalasin B." *Proc Natl Acad Sci U S A* 79(17): 5327-5331.
- Pineda, B., M. d. M. Saniger, et al. (2009). "Solid-phase assay for the detection of varicella zoster virus." *Future Virology* 4(6): 543-551.
- Pourati, J., A. Maniotis, et al. (1998). "Is cytoskeletal tension a major determinant of cell deformability in adherent endothelial cells?" *Am J Physiol* 274(5 Pt 1): C1283-1289.

- Putman, C. A., K. O. van der Werf, et al. (1994). "Viscoelasticity of living cells allows high resolution imaging by tapping mode atomic force microscopy." *Biophys J* 67(4): 1749-1753.
- Revenko, I. and R. Proksch (2000). "Magnetic and acoustic tapping mode microscopy of liquid phase phospholipid bilayers and DNA molecules." *J. Appl. Phys* 87(1): 526-533.
- Roos, W. H., K. Radtke, et al. (2009). "Scaffold expulsion and genome packaging trigger stabilization of herpes simplex virus capsids." *Proc Natl Acad Sci U S A* 106(24): 9673-9678.
- Sachse, C., J. Z. Chen, et al. (2007). "High-resolution electron microscopy of helical specimens: a fresh look at tobacco mosaic virus." *J Mol Biol* 371(3): 812-835.
- Schindler, H., D. Badt, et al. (2000). "Optimal sensitivity for molecular recognition MAC-mode AFM." *Ultramicroscopy* 82(1-4): 227-235.
- Schneeweiss, M. A. and I. Rubinstein (2007). *Metal Substrates for Self-assembled Monolayers. Encyclopedia of Electrochemistry, Wiley-VCH Verlag GmbH & Co. KGaA.*
- Shen, X. C., L. Bao, et al. (2011). "A simple and effective sample preparation method for atomic force microscopy visualization of individual DNA molecules in situ." *Mol Biol Rep* 38(2): 965-969.
- Siedlecki, C. A. and R. E. Marchant (1998). "Atomic force microscopy for characterization of the biomaterial interface." *Biomaterials* 19(4-5): 441-454.
- Straub, T. M., I. L. Pepper, et al. (1994). "Detection of naturally occurring enteroviruses and hepatitis A virus in undigested and anaerobically digested sludge using the polymerase chain reaction." *Can J Microbiol* 40(10): 884-888.
- Suarez, T., M. J. Gomara, et al. (2003). "Calcium-dependent conformational changes of membrane-bound Ebola fusion peptide drive vesicle fusion." *FEBS Lett* 535(1-3): 23-28.
- Tan, Y. H., J. R. Schallom, et al. (2011). "Characterization of protein immobilization on nanoporous gold using atomic force microscopy and scanning electron microscopy." *Nanoscale* 3(8): 3395-3407.
- Tian, D., Y. Wang, et al. (2011). "A novel strategy for exploring the reassortment origins of newly emerging influenza virus." *Bioinformatics* 7(2): 64-68.
- Trache, A. and G. A. Meininger (2008). "Atomic force microscopy (AFM)." *Curr Protoc Microbiol* Chapter 2: Unit 2C 2.
- Volkening, J. D. and S. J. Spatz (2009). "Purification of DNA from the cell-associated herpesvirus Marek's disease virus for 454 pyrosequencing using micrococcal nuclease digestion and polyethylene glycol precipitation." *J Virol Methods* 157(1): 55-61.
- Wagner, P. (1998). "Immobilization strategies for biological scanning probe microscopy." *FEBS Lett* 430(1-2): 112-115.
- Wang, N. (1998). "Mechanical interactions among cytoskeletal filaments." *Hypertension* 32(1): 162-165.
- Weiland, J. J. and T. W. Dreher (1993). "Cis-preferential replication of the turnip yellow mosaic virus RNA genome." *Proc Natl Acad Sci U S A* 90(13): 6095-6099.

- Wickramasinghe, S. R., B. Kalbfuss, et al. (2005). "Tangential flow microfiltration and ultrafiltration for human influenza A virus concentration and purification." *Biotechnol Bioeng* 92(2): 199-208.
- Wool-Lewis, R. J. and P. Bates (1999). "Endoproteolytic processing of the ebola virus envelope glycoprotein: cleavage is not required for function." *J Virol* 73(2): 1419-1426.
- Zhao, Q., Y. Wang, et al. (2006). "Maturation of recombinant hepatitis B virus surface antigen particles." *Hum Vaccin* 2(4): 174-180.



## **Atomic Force Microscopy Investigations into Biology - From Cell to Protein**

Edited by Dr. Christopher Frewin

ISBN 978-953-51-0114-7

Hard cover, 354 pages

**Publisher** InTech

**Published online** 07, March, 2012

**Published in print edition** March, 2012

The atomic force microscope (AFM) has become one of the leading nanoscale measurement techniques for materials science since its creation in the 1980's, but has been gaining popularity in a seemingly unrelated field of science: biology. The AFM naturally lends itself to investigating the topological surfaces of biological objects, from whole cells to protein particulates, and can also be used to determine physical properties such as Young's modulus, stiffness, molecular bond strength, surface friction, and many more. One of the most important reasons for the rise of biological AFM is that you can measure materials within a physiologically relevant environment (i.e. liquids). This book is a collection of works beginning with an introduction to the AFM along with techniques and methods of sample preparation. Then the book displays current research covering subjects ranging from nano-particulates, proteins, DNA, viruses, cellular structures, and the characterization of living cells.

### **How to reference**

In order to correctly reference this scholarly work, feel free to copy and paste the following:

Norma Hernández-Pedro, Edgar Rangel-López, Benjamín Pineda and Julio Sotelo (2012). Atomic Force Microscopy in Detection of Viruses, Atomic Force Microscopy Investigations into Biology - From Cell to Protein, Dr. Christopher Frewin (Ed.), ISBN: 978-953-51-0114-7, InTech, Available from:  
<http://www.intechopen.com/books/atomic-force-microscopy-investigations-into-biology-from-cell-to-protein/atomic-force-microscopy-in-detection-of-virus->

**INTECH**  
open science | open minds

### **InTech Europe**

University Campus STeP Ri  
Slavka Krautzeka 83/A  
51000 Rijeka, Croatia  
Phone: +385 (51) 770 447  
Fax: +385 (51) 686 166  
[www.intechopen.com](http://www.intechopen.com)

### **InTech China**

Unit 405, Office Block, Hotel Equatorial Shanghai  
No.65, Yan An Road (West), Shanghai, 200040, China  
中国上海市延安西路65号上海国际贵都大饭店办公楼405单元  
Phone: +86-21-62489820  
Fax: +86-21-62489821

© 2012 The Author(s). Licensee IntechOpen. This is an open access article distributed under the terms of the [Creative Commons Attribution 3.0 License](#), which permits unrestricted use, distribution, and reproduction in any medium, provided the original work is properly cited.